

1

2 INTEGRATING DYNAMIC PLANT GROWTH MODELS AND 3 MICROCLIMATES FOR SPECIES DISTRIBUTION MODELLING

4

Rafael Schouten, Peter A. Vesk and Michael R. Kearney

5 0.1 ABSTRACT

6 Climate is a major factor determining the distribution of plant species. Correlative models
7 are frequently used to model the relationships between species distributions and climatic
8 drivers but, increasingly, their use for prediction in novel scenarios such as climate change
9 is being questioned. Mechanistic models, where processes limiting plant distribution are
10 explicitly included, are regarded as preferable but more challenging.

11 The availability of tools for simulating microclimates with high spatial and temporal def-
12 inition has also opened new possibilities for simulating the limiting environmental stresses
13 experienced by plant over their ontogeny. However, the field of mechanistic species distri-
14 bution modelling is relatively new and the tools and theory for constructing these models
15 are underdeveloped.

16 In this paper we explore the potential for using a Dynamic Energy Budget model of
17 organism growth integrated with microclimate and photosynthesis models. We model the
18 interactions of plant growth and microclimatic stressors over the life stages of plant growth,
19 and scale them up to demonstrate predictions of distribution at the continental scale. We
20 develop the model using Julia, a new language for scientific computing, as a set of generic
21 modelling packages. These have a modular, toolkit structure that has the potential to
22 increase the efficiency and transparency of developing mechanistic SDMs.

23 0.2 INTRODUCTION

24 The relationship between the growth and distribution of plants and environmental drivers
25 is a fundamental concern of ecology (Billings 1952). Modern tools and datasets enable
26 modelling of the dynamic interactions between organisms and the environment at the scale
27 of the individual organism. This capability can be used to develop insights and hypotheses
28 about the mechanistic drivers of plant growth and stresses that limit the distribution of
29 plant species. The use of such a physiological approach may assist the prediction of species
30 distributions in future climates, or novel conditions (Bozinovic & Pörtner 2015; Kearney &
31 Porter 2009).

32 Species distribution models (SDMs) are often developed using correlative techniques,
33 with coarse-grained environmental predictors. However, there is a growing consensus that
34 ecological models need to incorporate more structural realism (Grimm & Berger 2016).
35 For this reason process-based, mechanistic and hybrid models have been proposed as a
36 more realistic alternative to correlative SDMs (Dormann et al. 2012; Kearney, Wintle
37 & Porter 2010; Singer et al. 2016; Connolly et al. 2017). Practically, correlative and
38 mechanistic models exist on a spectrum of increasing causal detail (Dormann et al. 2012),

39 where mechanistic models include explicit biophysical and physiological processes (Connolly
40 et al. 2017).

41 However, choosing mechanistic models over correlative models is not simply a question
42 of theoretical value, but also one of economy: mechanistic models are more difficult to
43 construct, and more computationally intensive than correlative models (Dormann et al.
44 2012; Kearney, Wintle & Porter 2010). Improvements to mechanistic species distribution
45 modelling require simultaneous development of theory and the practical tools for applying
46 it efficiently (Briscoe et al 2019).

47 *Mechanistic species distribution models for plants*

48 Mechanistic SDMs have become more common for animals (Kearney & Porter 2009). Al-
49 though mechanistic modelling has a longer history in plant biology (Grimm & Berger 2016),
50 mechanistic SDMs remain less well-developed for plants. We follow Connolly et al. (2017)
51 and distinguish mechanistic models from process-based models (PBMs), ignoring those that
52 include only dispersal processes without specifying the components of plant growth (Merow
53 et al. 2011).

54 A range of mechanistic models have been used to predict species distributions. These
55 include phenological models that integrate environmental stress factors (Morin, Viner &
56 Chuine 2008; Chuine & Beaubien 2001; Chapman et al. 2014) and models of environmental
57 interactions with growth processes based on tree growth rings (Sánchez-Salguero et al.
58 2016). Other models have incorporated plant growth and C/N allocation in response to
59 environmental drivers, to produce maps of relative growth potential (Higgins et al. 2012;
60 Higgins & Richardson 2014; Moncrieff et al. 2016; Storkey et al. 2014; Nabout et al. 2012).
61 Mechanistic growth models provide the most scope for capturing the interactions between
62 plant ontogeny and the environment, as plant stresses can co-occur in sequential patterns
63 with different effects across plant ontogeny (Niinemets 2010). They can also provide a
64 base model that can integrate phenological components, or be used for truly mechanistic
65 demographic and distribution models.

66 A key example of a mechanistic growth model used for SDMs is the Thornley Transport
67 Resistance model (TTR) (Thornley 1972a), that tracks carbon and nitrogen budgets for
68 roots and shoots. It has been used in hybrid mechanistic/fitted plant SDMs (Higgins et al.
69 2012; Higgins & Richardson 2014; Moncrieff et al. 2016). Additionally, Nabout et al. (2012)
70 applied the Plantgro model to maize distribution, which uses growth response curves tuned
71 to monthly conditions. Stratonovitch, Storkey & Semenov (2012) and Storkey et al. (2014)
72 used climatic data with daily time-steps and incorporated ontogeny in a sophisticated plant
73 SDM. However, the Sirius model (Jamieson et al. 1998) used in Storkey et al. (2014) is
74 focused on agricultural plants, and its formulation was not made available.

75 *Plant growth and Microclimate*

76 Realism in growth models can be increased by modelling causal processes more explicitly. It
77 can also be improved by using finer grained environmental variables, because the responses
78 of organisms to changes at the macroclimate scale actually occur at the microclimate scale
79 (Harwood, Mokany & Paine 2014).

80 Animals usually exercise some choice over the microclimates they are exposed to, but
81 the life of a plant occurs in a fixed location: they must tolerate all environmental conditions
82 that occur there over their lifespan. However, at a finer scale plants grow through vertical

83 climatic gradients over their ontogeny. They experience different conditions at different
84 life-stages, and these differences can be critical in growth process (Niinemets 2010) and
85 in constraining the boundaries of their distribution (Smith et al. 2009). To establish
86 at a particular location, plants must experience a favourable sequence of microclimatic
87 conditions that match the needs of all life stages – not simply favourable climatic averages.

88 Growth based plant SDMs have generally used long time-steps (i.e. monthly) and cli-
89 matic, rather than microclimatic data (Nabout et al. 2012; Higgins et al. 2012; Higgins &
90 Richardson 2014; Moncrieff et al. 2016). A general plant model suitable for SDMs – that
91 can simulate complete plant ontogeny with realistic combinations of environmental stresses
92 – remains to be demonstrated. Dynamic energy budget (DEB) growth models, coupled to
93 mass and energy exchange between organisms and their microclimates, have achieved this
94 for animal SDMs (Kearney 2012; Kearney et al. 2018).

95 *Dynamic Energy Budget theory*

96 Dynamic Energy Budget theory (DEB) generalises growth processes for all organisms and
97 symbioses (Kooijman 2010). It is frequently used to model the transition from juvenile to
98 adult in animals and bacteria (Sarà et al. 2013; Jager, Martin & Zimmer 2013) and can
99 capture complete organismal ontogeny. It has been used to model animal species distribu-
100 tions (Kearney 2012; Kearney et al. 2018), and has been suggested as an alternative growth
101 model for plant SDMs (Higgins et al. 2012).

102 DEB theory simplifies the metabolism of organisms to material fluxes of substrates in
103 processes of assimilation, growth and dissipation (Lorena et al. 2010). From simple rules
104 and feedbacks it can capture complex growth dynamics while being explicit about matter,
105 energy and entropy balances (Sousa et al. 2010).

106 DEB models focus on the interactions of different abstract categories of biomass, namely:
107 *structure* (V), that is produced by the growth process and requires ongoing maintenance,
108 and *reserve* (E), that represents the pool into which assimilates flow, and does not require
109 maintenance. An additional type is *product* (P), representing byproducts of the growth
110 process. In animals these are often excreted, but in plants may be included in measured
111 biomass as bark and heartwood. The simplifying assumption of this framework is that each
112 category has fixed proportion of chemical constituents. This enables the closure of both
113 mass and energy balances (Sousa et al. 2010).

114 For models with multiple reserve substrates, such as separate carbon and nitrogen re-
115 serves, “synthesizing units” (SUs) are used to model enzyme dynamics for reserve combi-
116 nation, giving smooth transitions between limiting resources (Ledder et al. 2019; Kooijman
117 2010, pp.99–105). Synthesizing units bind multiple substrates to synthesize compounds,
118 depending on their availability. Using an SU, carbon and nitrogen pools can be combined
119 into a general reserve to be used in growth and maintenance. Reserve mobilised in each
120 simulation time-step is calculated from the ratio of reserve to structure, adjusting growth
121 rates to match available resources.

122 A useful outcome of the reserve-structure dynamics of a DEB model that tracks nutrient
123 state is the ability to model growth from embryo to mature organism, by initially allocating
124 high reserve/structure ratios and small structural mass. This can produce smooth tran-
125 sitions from the embryo phase, dependent primarily on stored nutrients, to later phases
126 where nutrients are assimilated from the environment. Previous models of plant ontogeny
127 often start with a seedling (Levy et al. 2000). In DEB models, growth rates vary with
128 temperature but also with the dynamics of the root and shoot reserves, the growth rate

129 being proportional to the density of the limiting reserve. This captures transient dynamics
130 that drive, for example, rapid growth of seedlings or rapid shoot growth after a sudden loss
131 of biomass from e.g. grazing events or fire.

132 The intrinsic generality and modularity of DEB theory means that, in principle, any
133 number of structures can interact to exchange substrates, allowing simulations of single-
134 celled heterotrophs, complex autotrophs, and even symbioses. This ability allows us to
135 construct a DEB plant model, where at least root and shoot structures must be considered
136 explicitly to model asynchronous nutrient assimilation. It also means that a DEB model has
137 the open-ended potential to model more or less complex dynamics, by adding or removing
138 structures. We could represent stems, leaves and roots separately, or including substrate
139 exchange between fine roots and soil symbionts – requiring few additional formulations or
140 parameters.

141 *DEB models for plants*

142 While the DEB model was proposed as a framework for modelling all organisms, the major-
143 ity of published DEB models have focused on heterotrophs. The literature for autotrophs
144 remains sparse: Lorena et al. (2010), Kooijman (2010), Muller et al. (2009) Kooijman,
145 Andersen & Kooij (2004); Livanou et al. (2018) and Ledder et al. (2019) are notable contri-
146 butions. A simple, single-structure microalgae model was presented in Lorena et al. (2010),
147 contrasting with most animal models by tracking separate reserves for carbon and nitrogen
148 to model temporally separated uptake dynamics. The symbiosis of a simple heterotroph
149 and photo-autotroph was also modeled by Muller et al. (2009).

150 Modelling plants requires multiple structures to capture the additional spatial separa-
151 tion of nutrient and carbon uptake that occurs in roots and shoots (Kooijman 2010,
152 pp.201–206). Such a plant model was demonstrated by Kooijman (2010). However, it has
153 not been widely tested or peer-reviewed and uses a large number of parameters. Recently
154 Ledder et al. (2019) explored the dynamics of a simplified two-structured plant model,
155 proposing “The local control theory of resource allocation”. In this formulation, resource
156 sharing between plant structures is similar to resource sharing in a holobiont: roots and
157 shoots only translocate unused metabolites, without centralised coordination or fixed al-
158 locations to translocation. This simple formulation achieves optimal growth rates, while
159 maintaining dynamic growth behaviour. It also requires fewer parameters and causal pro-
160 cesses than either globally-optimised resource sharing or the fixed-proportion local control
161 used in Kooijman (2010) and in the well known Thornley Transport Resistance plant growth
162 model (TTR) (Thornley 1972a).

163 There are some differences in the strategies used to track carbon, nitrogen and general
164 reserve state in DEB autotroph models. Kooijman (2010) tracked carbon reserve (C), nitro-
165 gen reserve (N) and general reserve (E), while Ledder et al. (2019) did not track reserves at
166 all, instead generating general reserve from assimilated C and N for each time-step. Lorena
167 et al. (2010) track C and N reserves. Despite structural differences, these models invariably
168 track reserve and structure as abstract, but stoichiometrically fixed compounds measured
169 in C moles and N moles.

170 *Modelling Microclimates*

171 Improvements in climatic datasets and downscaling methods have enabled detailed mod-
172 elling of microclimate at the scale of individual organisms in any location. NicheMapR

173 (Kearney & Porter 2017) and the microclimate datasets (Kearney 2018) generated by it are
174 tools that make detailed site-specific microclimates accessible over multiple decades, with
175 the hourly resolution for multiple heights and depths at reasonable accuracy. They provide
176 soil water potential (Kearney & Maino 2018), soil temperature (Kearney et al. 2014), in-
177 cident radiation, air temperature, snow cover, relative humidity and wind-speed, enabling
178 the modelling of finely detailed organism-environment interactions. Microclimate data are
179 provided as hourly sequences of environmental variables in discrete spatial layers.

180 *Connecting growth models and microclimates*

181 DEB models do not represent organism growth spatially, besides simple surface area/mass
182 relationships. But microclimates are fundamentally spatial. Water availability and soil
183 temperature both vary with depth, while air temperature varies with height above ground.
184 This means that a spatially-explicit model is required to integrate a DEB growth model
185 with microclimate data.

186 The interactions of plant growth and microclimate could be most accurately modelled
187 with three-dimensional models of root and shoot architecture (Vrugt et al. 2001). However,
188 producing mapped species distributions imposes a number of practical constraints. There
189 are limits to computing power when models may run over 8000 times for a year of growth
190 at a single point. This can translate to the order of a billion runs to produce continent-scale
191 maps on decennial timescales. Further, our ability to easily construct complex models and
192 determine their parameters is limited by the availability of easily assembled modelling tools
193 and data. The dimensionality and accuracy of the spatial transformation used must be
194 some compromise between these factors.

195 *Realistic behaviour of a DEB plant model*

196 There are a number of requirements for our plant growth model. Generally, a plant model
197 should to some extent balance the growth of roots and shoots to align with their relative
198 needs for substrate assimilation. To enable the modelling of growth throughout life-stages,
199 it should capture growth trajectories from seed to plant, switching smoothly between stored
200 and assimilated resources.

201 *Optimal partitioning*

202 Optimal partitioning theory (Thornley 1972a; McCarthy & Enquist 2007a) describes how
203 resources are optimally allocated between plant organs depending on relative availability;
204 plants with adequate N supplies preferentially grow more shoots, instead of roots. This
205 dynamic is a central component of many plant models (Cheeseman 1993; Ledder et al.
206 2019), although it is not without criticism (Lambers 1983; Müller, Schmid & Weiner 2000).

207 There are multiple methods for modelling optimal root/shoot ratios. Two alternatives
208 are *central* (Perrin 1992) and *local* (Cheeseman 1993; Ledder et al. 2019) control of translo-
209 cation. Cheeseman (1993) showed that simple local rules can lead to the emergence of bal-
210 ancing at the scale of the whole plant, without the need to invoke signalling or centralised
211 control of allocation. However, they use fitted polynomial functions for growth rates, rather
212 than bottom-up methods that could respond to hourly microclimate conditions. Ledder et
213 al. (2019) recently demonstrated a local control model in a context of dynamic growth
214 using the synthesising units of a two-substrate DEB model, where translocation of excess
215 metabolites achieves optimal balanced growth.

216 Shoots low in C translocate less or no excess to roots, leading to more shoot growth
217 than root growth, until balance is achieved. The inverse happens for N in roots. With
218 parallel complementary SUs a proportion of each substrate is always translocated, and
219 effectively cycled between structures. These dynamics can be fine-tuned by using k-family
220 synthesizing units, where the overall proportions of used and rejected metabolites can be
221 adjusted (Ledder et al. 2019).

222 One difference between local control theory and functional-balance theory is that root
223 growth is not affected by low water availability in the version of local control presented in
224 Ledder et al. (2019). Optimisation of water uptake is not always supported by experimental
225 results (Metcalfé et al. 2008; McConnaughay & Coleman 1999a) and root/shoot ratios may
226 be unaffected by water availability (McConnaughay & Coleman 1999b). However, other
227 studies cite both water and nutrients as factors in optimal root/shoot scaling. (McCarthy
228 & Enquist 2007b). In local control theory (Ledder et al. 2019) only substrate availability
229 (generally C and N) affect root/shoot ratios. Water shortages may have indirect effects by
230 limiting assimilation.

231 *Seed/plant transitions*

232 Modelling complete plant ontogeny and changes in relation to microclimatic stresses requires
233 a smooth transition between seed and plant life-stages. However, this transition is not
234 commonly modelled. Seeds are largely composed of reserves such as carbohydrate and lipids,
235 and rapid initial growth can be driven by the high ratio of reserve to structural tissue. DEB
236 theory is well suited to modelling these processes, because the reserve concept links the
237 embryo to the life cycle through the transition from use of initial reserve to assimilation of
238 additional reserve (Kooijman 1986). Periods of slowdown and readjustment of growth rates
239 may occur in the transition between seed reserve and assimilated reserve when resources
240 are limiting (Kitajima 2002). These can be captured by a DEB model.

241 *Aims*

242 In this paper, we aim to explore the potential for modelling plant distributions based on
243 limits to plant growth caused by the specific sequence of stresses a plant experiences during
244 its ontogeny. There are three components of this approach. First, developing practical
245 modelling tools that support both our current aims and future research in the field; second,
246 developing methods to connect a mechanistic model of plant ontogeny to microclimate
247 models; and third, assessing the behaviour of the model across plant ontogeny and varying
248 environmental conditions and scenarios, up to the scale of continental distribution. Ulti-
249 mately, these components are intended to collectively enable the parametrisation of species
250 distribution models of plant species and functional groups.

251 To model plant ontogeny with fine spatial and temporal resolution, we use a DEB
252 model and connect assimilation, growth and maintenance processes to the microclimOz
253 microclimate data set (Kearney 2018) using temperature response curves and a photosyn-
254 thesis/transpiration model. We develop model components as separate libraries that enable
255 future adaption for use in a wide variety of SDMs, and in ecological models more generally.

256 0.3 METHODS

257 We modelled a simple, generalised C3 grass or herb-like plant using a two-structure two-
258 reserve DEB model. The DEB model is based on the plant model provided in Kooijman
259 (2016) and Kooijman (2010) with simplifications outlined by Ledder et al. (2019) and Lorena
260 et al. (2010). While the plant model in Kooijman (2016) specifies a photosynthesis compo-
261 nent for C assimilation, it does not integrate environmental variables, stomatal conductance
262 or the role of soil moisture in C uptake. Instead we use a Farquhar-von Caemmerer-Berry
263 photosynthesis, stomatal conductance and soil moisture and model adapted from MAESPA
264 (Duursma & Medlyn 2012).

265 We implemented the model in Julia (Bezanson et al. 2012), a programming language
266 developed for scientific computing, that enables the performance of C or Fortran languages
267 with the modularity and ease of use of Python or R. DEB, photosynthesis, and microcli-
268 mate integration packages were implemented as the standalone, modular libraries Dynam-
269 icEnergyBudgets.jl (<https://github.com/rafaqz/DynamicEnergyBudgets.jl>), Photosynthe-
270 sis.jl (<https://github.com/rafaqz/Photosynthesis.jl>) and Microclimate.jl (<https://github.com/rafaqz/Microclima>)
271 These provide generalised interfaces that facilitate adaptation for many modelling pur-
272 poses (including outside of SDMs and ecology). Julia’s type-system and multiple-dispatch
273 paradigm allowed us to include most components and parameters as interchangeable or op-
274 tional. This improves interactive exploration, allowing easy reduction of model parameter
275 number but also addition of components for alternate formulations. Model components are
276 compiled together by Julia at run-time to produce computational performance in the order
277 of lower-level languages like C or Fortran.

278 *State variables*

279 Tracking nutrient reserves allows modelling of seed reserve and scenarios with fluctuating
280 assimilation rates, as are common with variable environmental conditions. To allow this,
281 we followed the approach of Lorena et al. (2010), tracking structure V with C and N
282 reserves, but calculating general reserve at each time-step. These three state variables for
283 roots and shoots lead to a six-state model, consistent with traditional plant models such as
284 TTR (Thornley 1972b) and SIMPLE (Cheeseman 1993).

285 The modular DEB formulation allows for inclusion of additional state variables such
286 as P (production) and M (maturity). P can track the production of growth byproducts
287 such as leaf litter, or bark and heartwood in woody plants, while M can track reproductive
288 maturity and seed-set.

289 We allocate initial seed mass by assigning large C and N with small V (Table 1). If
290 initial reserve masses assigned to shoot and root do not match the ratio of later assimi-
291 lation rates, balancing oscillations occurred between root and shoot growth until a stable
292 assimilation ratio is reached. These oscillations drove early model “death” in variable con-
293 ditions. We therefore used an initial reserve structure ratio that matches later shoot/root
294 ratio of 4:1, minimising early growth-rate oscillations. Plants were simulated to grow for
295 six months starting at monthly intervals over the six year period from January 2005 to De-
296 cember 2010. We use microclimates simulated from historical climatic data from 2005-2011
297 (Kearney 2018), covering the ‘millennium’ drought (Dijk et al. 2013) and the return of
298 wetter conditions from late 2009.

Table 1: Initial masses of reserve and structure

State	Symbol	Mass (mg)
Shoot Structure	V_S	0.2
Shoot C Reserve	C_S	5.0
Shoot N Reserve	N_S	0.2
Root Structure	V_R	0.04
Root C Reserve	C_R	1.0
Root N Reserve	N_R	0.04

299 *Avoiding Over-parametrization*

300 The usefulness of complex, over-parameterised ecological models is debatable (Reichert &
301 Omlin 1997). The DEB plant model in Kooijman (2016)] has 60-80 parameters depending
302 on the use case and interpretation, reflecting the potential biologically-relevant complexity
303 in a multi-state model. Microclimate integration requires additional parameters, while the
304 MAESPA photosynthesis model itself has many parameters (20-40). This combination
305 could result in a model that is over-parametrized and difficult to reason about, to explore
306 and ultimately to parametrize. However, a DEB plant model can be simplified in two
307 ways: amalgamation of parameters across structures and substrates, and simplification of
308 the formulation.

309 Amalgamation of parameters is possible if we assume that there are common parameters
310 shared between root and shoot structures, and for rates of substrate turnover. Kooijman
311 (2010) used three \dot{k} parameters per structure for the turnover of each reserve. Lorena et
312 al. (2010) used only a single \dot{k} parameter, as mobilisation rates were deemed to be the
313 same in algae. Practically, this simplifies interactive control over whole plant turnover
314 rates, and reduces failure of simulations due to fluctuations induced by differences between
315 \dot{k} parameters. For similar reasons we also amalgamated parameters for maintenance, yield
316 for conversion of reserve to structure, and N/C ratios of all reserve and structure state.

317 Performing sensitivity analysis on model components and parameters is an obvious ana-
318 lytical approach to parameter reduction. However, it did not prove to be as easy as typical
319 sensitivity analysis of ecological models. The influence some parameters is highly dependent
320 on microclimatic conditions; sensitivity can be calculated for one particular microclimatic
321 context, but this may not be useful for understanding how the model behaves across a wider
322 range of environments. Running sensitivity analysis across a dataset such as microclimOz
323 is a potential solution, but is computationally intensive and was not attempted here.

324 Instead we focused on manual sensitivity analysis. To facilitate this we developed a
325 user-interface that dynamically updates simulations as parameter values are changed. The
326 modular formulation also allowed us to swap or remove whole components from the interface
327 to compare their behaviour in different environments.

Table 2: Model Components

Component	Formulation(s)	Shared/Spec	Parameters
Core (inc. growth + maint)		Shared	7
SU	Parallel Complimentary	Shared	0
Product	None	Specific	Unused

Table 2: Model Components

Component	Formulation(s)	Shared/Spec	Parameters
Maturity	None	Specific	Unused
Resorption	Lossless	Shared	1
Rejected translocation	Lossless	Specific	0, 0
Fixed translocation	None	Specific	Unused
Assimilation	FvCB, Constant N	Specific	
Scaling	Plant Morph	Specific	2, 2
Allometry	Allometry	Specific	2, 2

328 Formulation changes achieved using this method included simplification of growth rate
329 calculations to use only two reserve substrates, and removing proportional translocation,
330 following Ledder et al. (2019). Additionally, for plants without bark or heartwood, product
331 is not a component of measured biomass. Product is also inherently modular in DEB, as
332 it is a proportion of otherwise lost reserves. It could thus be ignored. In our case the
333 reproductive phase of the life cycle is of less interest, and maturity and reproduction was
334 also be ignored. However, to allow the optional use of maturity and the fixed translocation
335 of the original model, we redefined the fraction of available flux directed to growth κ_{soma} ,
336 as a function of the components of a structure s :

$$\kappa_{soma}(s) = 1 - \kappa_{maturity}(s) - \kappa_{translocation}(s) \quad (1)$$

337 In our simplified formulation, κ_{soma} is equal to 1.

338 For simplicity, we also ignore the complexities of nitrogen assimilation and scale N uptake
339 on the basis of root mass, the minimum requirement to simulate root/shoot balancing
340 dynamics.

341 Kooijman (2010) used parameters for germination size and switches that initiate C and
342 N assimilation at some point after growth has begun. This produces switching artefacts in
343 early growth dynamics, and requires a parameter for each structure. In our formulation,
344 photosynthesis and nitrogen uptake began from the start of the simulation, when the plant
345 is still a seed. The structural mass of a seed is small in proportion to the reserve mass, and
346 assimilation in early growth is not significant in comparison to reserve mobilisation (Fig. 2).

347 In combination, these changes reduced DEB model parameters from approximately 70
348 to 13 (not including environment or photosynthesis components), and reduced complexity
349 without significant loss of dynamic capability. This simplified exploration of the model's
350 behaviour, while allowing flexibility to increase complexity where necessary. The final model
351 configuration is demonstrated in fig. 1.

352 *Microclimate integration*

353 Integrating a DEB plant growth model with microclimate data requires connecting spatially
354 implicit masses of the DEB structures to the spatial distribution of environmental conditions
355 in the microclimate.

356 In this section we describe how we used allometric equations to connect plant structures
357 to microclimates, and how temperature response and assimilation formulations were used to
358 connect variables to growth processes. We also describe a resorption formulation to balance
359 available reserve and maintenance requirements in fluctuating microclimatic conditions.

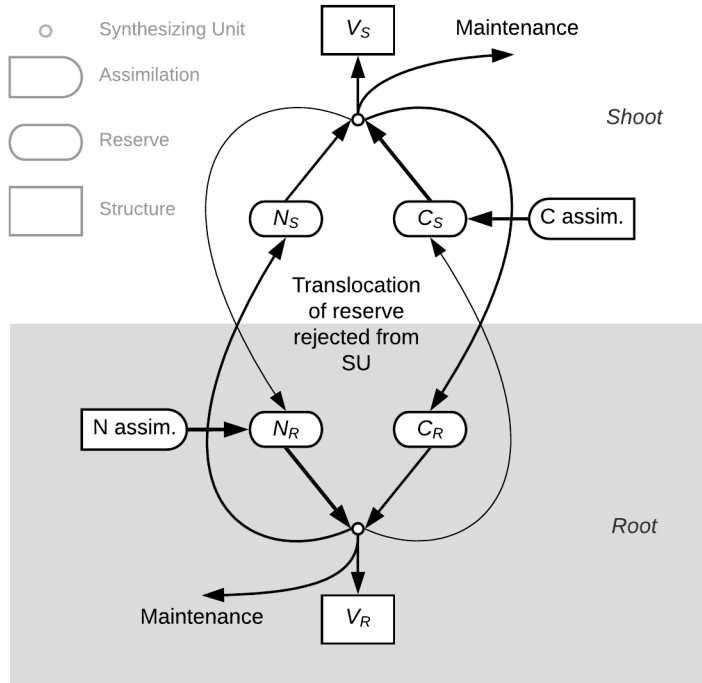


Figure 1: Diagram of the simplified DEB plant model. C and N are assimilated into C_S and N_R reserves using abstracted assimilation components. Mobilised reserves are incorporated into root and shoot structure, V_R and V_S , via synthesising units (circles). Substrate rejected from this process is translocated bidirectionally between roots and shoots. In practice far more N is translocated from root to shoot, and C from shoot to root, but cycling does occur.

360 *Allometry*

361 For any given geographic location, microclimOz data varies in only one (vertical) dimension
 362 at the microclimate scale, if variation in shade cover is ignored. We modelled only this
 363 vertical dimension, calculating the depth of roots and the height shoots for a given structural
 364 mass. To estimate these, a simple allometric equation was used:

$$\beta_1 (mass - \beta_0)^\alpha \quad (2)$$

365 Where β_0 is the intercept (mass at the soil surface), β_1 is a scalar and α the exponent. β_0
 366 was set to the initial seed mass, for a seed close to the soil surface. Microclimate values
 367 used in the simulation are interpolated between available height/depth layers.

368 *Photosynthesis*

369 In DEB models each reserve requires an assimilation process (Kooijman 2010, p. 206).
 370 We defined assimilation processes as modular components external to the DEB framework,
 371 and used an external photosynthesis model to calculate C assimilation and modify shoot
 372 temperature.

373 The Farquhar-von Caemmerer-Berry (Farquhar, Caemmerer & Berry 1980; Caemmerer
 374 & Farquhar 1981) photosynthesis models are widely used in plant science, and an obvious

375 addition to a mechanistic plant model (Higgins et al. 2012). Developers of open-source mod-
376 els such as MAESPA (Duursma & Medlyn 2012) have put significant work into connecting
377 Farquhar photosynthesis and Ball-Berry derived stomatal conductance to environmental
378 drivers such as temperature and soil moisture. However, MAESPA was not written as a
379 multi-purpose photosynthesis library. We adapted components of MAESPA into a modu-
380 lar, general purpose library of photosynthesis, stomatal conductance and plant heat balance
381 formulations: Photosynthesis.jl. These formulations are extensive and will not be covered
382 in this paper, but are available in the source of Photynthesis.jl, and covered in (Duursma
383 & Medlyn 2012), noting that canopy and spatial components are not included in Photo-
384 synthesis.jl. We used the simple Ball-Berry stomatal conductance model, modified by an
385 exponential response to soil water potential. Our choice of model components and param-
386 eters is essentially arbitrary and purely for demonstration. We also used a non-stomatal
387 physiological response to soil water potential defined in (Zhou et al. 2013). Soil water
388 potential was taken to be the maximum that the root system can access across its ver-
389 tical extent. This formulation resulted in a ‘Carbon Starvation’ model of drought stress
390 (O’Grady et al. 2013).

391 *Temperature*

392 Physiological processes in plants are reduced by temperatures above or below some opti-
393 mum (Parent & Tardieu 2012). The plant model in Kooijman (2016) described 1, 3 and
394 5 parameter temperature response models. However, the lower parameter models do not
395 capture decreasing growth rates above an optimum temperature. A simpler two-parameter
396 model can adequately represent this temperature response for plants, and plant growth and
397 maintenance processes are corrected by the formulation from Parent & Tardieu (2012). We
398 used the provided parameter values for wheat.

399 Root temperature was taken as equal to the soil temperature at the midpoint of root
400 depth. Above-ground microclimate variables were interpolated at the midpoint of shoot
401 height. To calculate shoot temperature we include the effects of air temperature, relative
402 humidity, wind-speed and soil water potential by iteratively solving the photosynthesis/s-
403 tomatal conductance model, as in MAESPA.

404 For the present purpose, we ignored plant behaviours like changes in leaf angle (Karban
405 2008) or leaf thermoregulation (Michaletz et al. 2015).

406 *Nutrient resorption*

407 Plants regularly drop leaves and slough roots, with some resorption of nutrients (Wright
408 & Westoby 2003). This may occur more rapidly in stressful conditions (Munné-Bosch &
409 Alegre 2004). With highly variable microclimate data, simulations of a DEB plant model
410 frequently ended in plant death when growth rates fell below zero, due to lack of reserves
411 for structural maintenance. The capability to shed excess structure appears to be both
412 mechanistically realistic and a practical requirement of modelling dynamic plant growth in
413 variable microclimates.

414 The shedding of structure due to stress can be simulated by removing a proportion of
415 structural and reserve mass as a function of growth rate. As growth rate is determined
416 by resource availability after maintenance and temperature suitability, it is a reasonable
417 indicator of stress. Our formulation uses the simplified assumption that if a leaf or branch
418 is dropped, the reserve fraction is able to be reabsorbed, simply remaining in the reserve

419 state C and N , but structural components are not recoverable, and are subtracted from
 420 structural state V . We used a half-saturation point for metabolic rate that modulates the
 421 rate of resorption. Loss of mass is defined as:

$$jV = -V * \left(1 - \frac{1}{1 + \frac{h}{r}}\right) \quad (3)$$

422 where V is structure, j , change in structure, r is the growth rate, and h is the rate where
 423 half of the current structural mass will be lost per day. At $h = 0$ no loss of structure will
 424 occur, while at $h = \infty$ all structure will be lost for any rate r . The negative feedback
 425 induced by the dependency of the growth rate on the ratio of structure to reserve will mean
 426 r tends to remain significantly larger than h .

427 Plants often have imperfect and different rates of resorption of N and C (Vergutz et al.
 428 2012). This formulation is available in DynamicEnergyBudgets.jl, but has two additional
 429 parameters, and was not used here.

430 *Microclimatic Scenarios*

431 For plotting simulations of plant ontogeny, we used three microclimate scenarios along a
 432 latitudinal transect from the east coast of Australia, moving west (Table 3).

Table 3: Transect

Location	Long	Lat
T1	148.92	-31.80
T2	145.92	-31.80
T3	142.92	-31.80

433 We utilised the 8-layer datasets from MicroclimOz for soil temperature and soil water
 434 potential and two-layer datasets for air temperature, relative humidity and wind speed.
 435 Single-layer data was used for incident solar radiation. The datasets for zero percent shade
 436 were used for all simulations.

437 *Simulation*

438 A numerical integration was used, with a fixed hourly time-step to include all available
 439 microclimate data. It was performed for a six month period to model the ontogeny of an
 440 annual plant. Plant death occurred when either root or shoot growth rate dropped below
 441 zero.

442 We ran this six month simulation in each transect location over the six year period from
 443 2005 to 2010, starting at the beginning of each month. The model was then run for the
 444 entire grid of Australian microclimate data, starting at monthly intervals over the same six
 445 year period. The maximum shoot mass registered during each simulation was stored, and
 446 the mean taken from all simulations starting in each particular year.

447 Initially we plotted selected simulations at the first transect location, starting in August
 448 2005, to demonstrate the dynamics of the model.

449 0.4 RESULTS

450 The model smoothly simulated the early stages of plant ontogeny against a background of
451 microclimatic variation (fig. 2), transitioning from dependence on stored seed reserves to
452 assimilated reserves. A period of stalled growth and rebalancing was visible in late Septem-
453 ber when seed reserves became depleted, and low soil water potential limited assimilation
454 and growth until late October. As N uptake is not mediated by soil water potential in the
455 model, but C assimilation is, N assimilation was higher than C assimilation in dry times.
456 This caused root growth to halt during water stress due to high availability of N.

457 Plant growth rates were corrected for the effects of temperature above or below the
458 optimum (fig. 2). For roots this quickly stabilised as they grew to deeper soil levels with
459 more stable temperature regimes. In contrast, leaf temperature, and consequently growth
460 rate, fluctuated strongly throughout plant ontogeny.

461 *Temporal variation along a transect*

462 With increasing aridity moving inland along the transect between T1 and T3, the overall
463 proportion of plants surviving decreased (fig. 3). The end of the millennium drought can
464 be seen with improved recruitment rates in 2009 and 2010. At T2, A long sequence of high
465 vapour pressure deficit and soil water potential combined with moderate soil temperature
466 in 2010. This allowed simulations to accrue higher biomass than any simulations in T1.
467 Simulations at T3 had a similar spike in 2010, but overall growth was more constrained by
468 environmental stresses than at either T1 or T2.

469 *Projected Australian distribution*

470 The patterns seen in the transect are reflected across eastern Australia when simulated for
471 the entire MicroclimOz dataset (fig. 4). Significantly broader distributions are visible in
472 2009 and 2010 with a marked inland shift in maximum growth rates, as would be expected
473 with the end of the millennium drought. Fig. 4 also demonstrates that it is computationally
474 tractable to produce distribution maps from this model, using a consumer desktop computer.

475 0.5 DISCUSSION

476 In this paper we have demonstrated a proof of concept for a mechanistic, ontogenetically-
477 explicit plant species distribution model. A simple DEB model of plant ontogeny, coupled
478 to microclimatic drivers, can produce realistic plant growth dynamics from seed to maturity
479 that respond to multiple environmental stresses and generate plausible spatial distributions.

480 Fundamental to the development of this model was component-based design methodol-
481 ogy for mechanistic modelling. We have defined modular components that allowed us to
482 iteratively simplify the model, and this should facilitate further development of mechanistic
483 SDMs and other applications in the life-sciences.

484 However, it remains to be demonstrated that this class of models can fitted to spe-
485 cific species or functional groups with more predictive success than correlative models, or
486 simpler process-based models. Model-fitting methods, mechanistic growth scaling and mi-
487 croclimate/plant interactions are avenues of further research.

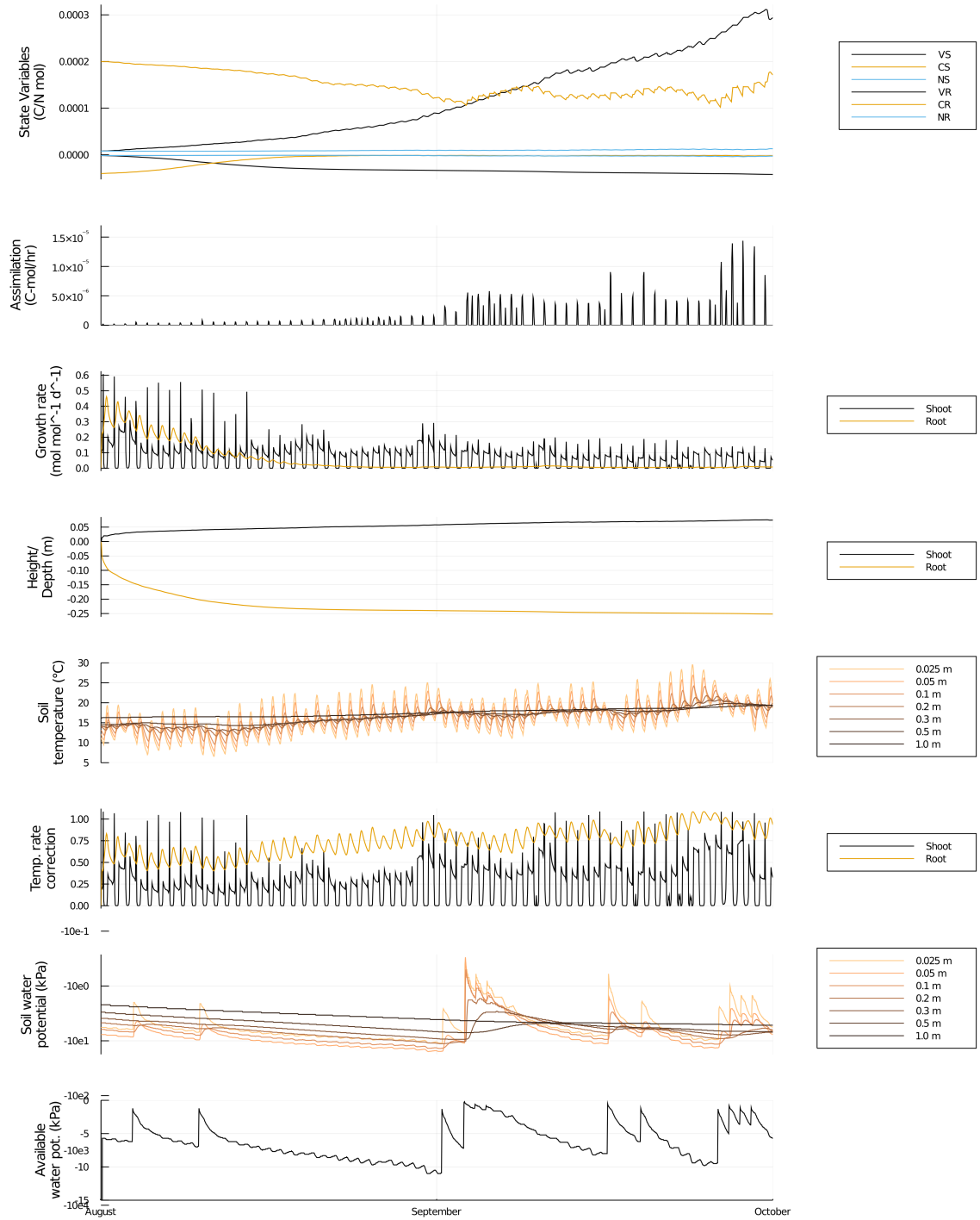


Figure 2: Early development in spring 2005 of at T1 in coastal NSW starting, showing detailed microclimate conditions and responses. Root state is shown as negative values. The calculated temperature correction factor and available soil water potential are shown in response to fixed environmental variables of soil temperature and water potential. This period demonstrates the transition between growth driven by seed reserve and by assimilated C and N.

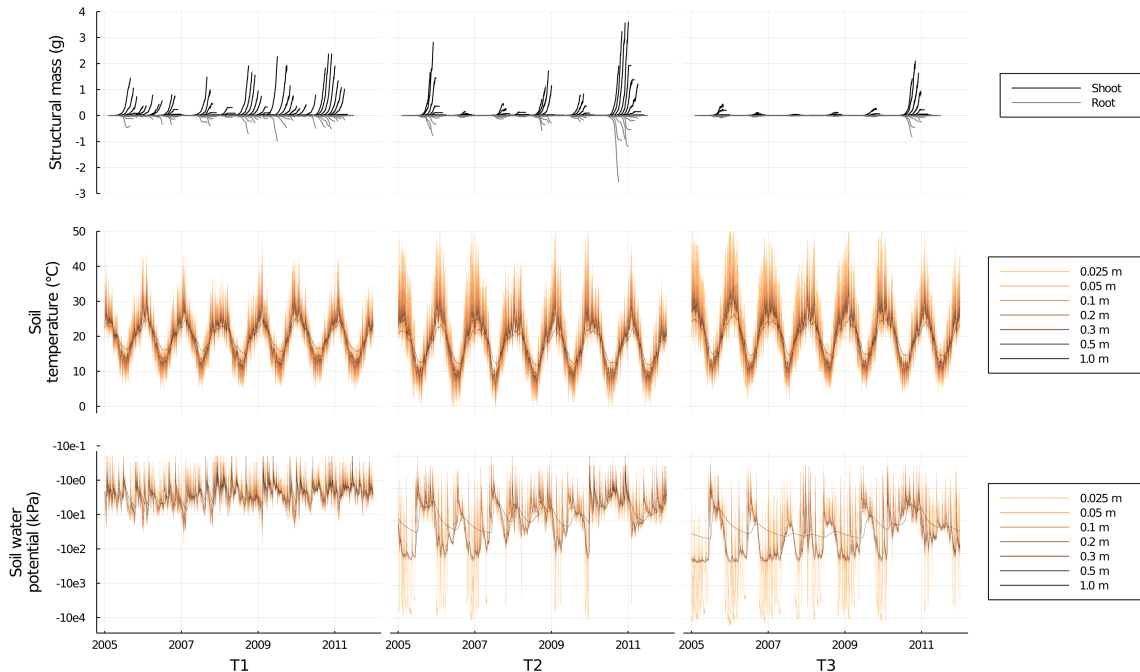


Figure 3: Six month simulations starting each month from 2001/2002 to 2010/2011, for all three locations. Growth plots show (dry) structural mass, here converted to grams. Root structural mass is shown as negative values. Soil water potential is shown on a log scale. A period of strong growth can be seen during 2010 in inland locations, coinciding with high soil water potential and moderate temperatures.

488 *Extensible modelling tools*

489 Mechanistic species distribution models are more difficult to build and more processor in-
 490 tensive than correlative models (Cabral, Valente & Hartig 2017; Connolly et al. 2017). The
 491 modelling packages that form the basis of this model outline a set of strategies for improv-
 492 ing this situation. We have demonstrated two distinct methods for extending the presented
 493 model: extensible structure of the core DEB model, and interchangeable physiological and
 494 climatic components.

495 *Modularity of structures and substrates in DEB*

496 The number of structures and substrates of a DEB model can be flexibly extended to suit
 497 the requirements of a problem, allowing open-ended exploration using the same theoretical
 498 framework and modelling tools. This has been demonstrated for use in both single- or
 499 two-structured models, with one or two substrates. However, models used in plant SDMs
 500 (Stratonovitch, Storkey & Semenov 2012; Storkey et al. 2014) and other purposes (Falster
 501 et al. 2016) use additional structures to model plant growth. This is likely to be a common
 502 requirement. Despite the capacity for multiple structures in DEB theory (Kooijman 2010,
 503 pp.180–188), a generalised computational framework for chaining more than two structures
 504 has been lacking. Chained structures require methods for partitioning translocation between
 505 both adjacent structures, such as the case of stems translocating resources between leaves
 506 and roots.

507 Additional reserve substrates such as phosphorus may also be added and tracked to

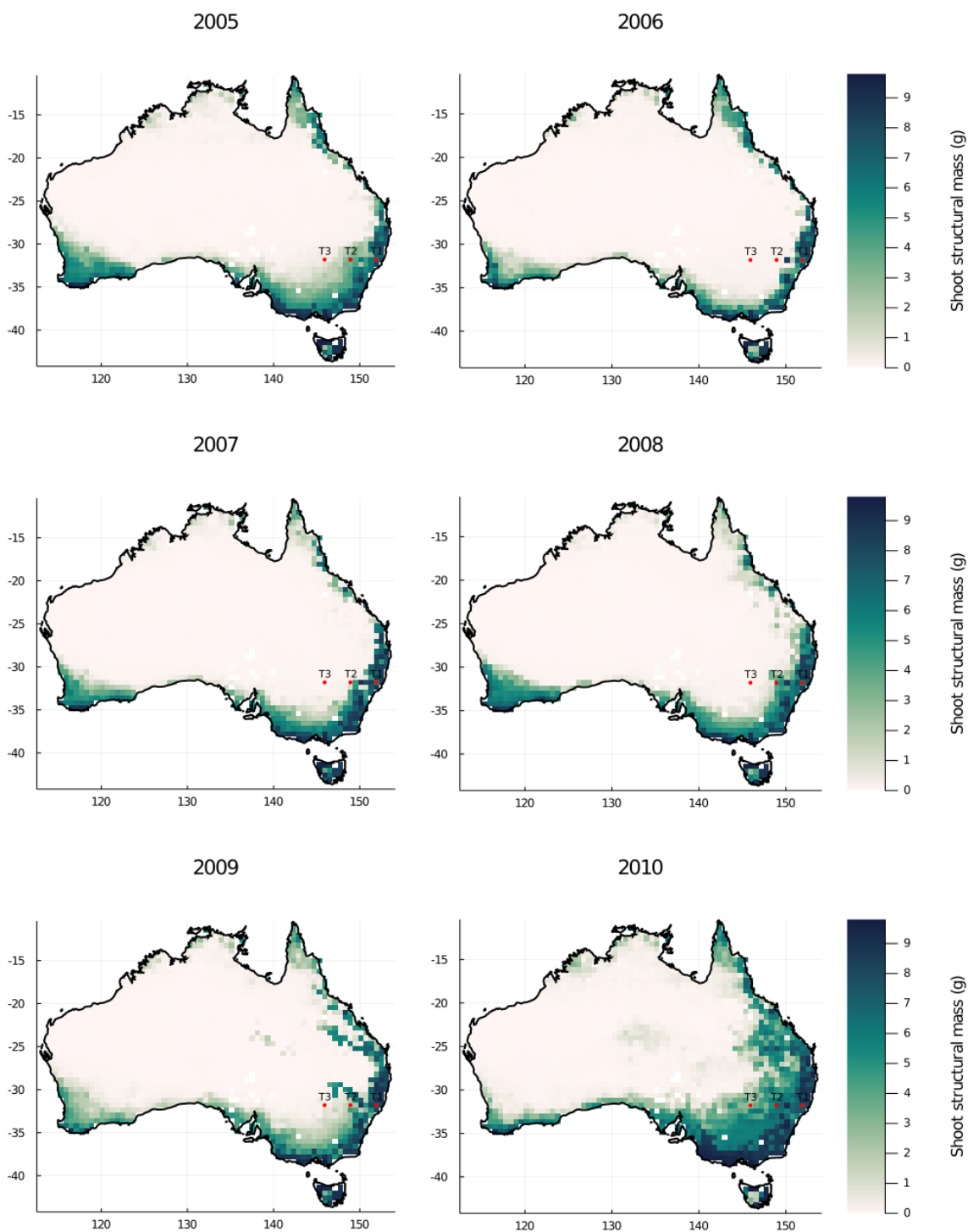


Figure 4: Distribution map of maximum plant growth. Maximum shoot mass from 12 six-month simulations, starting at the first day of each month, in each year. Simulations are run for the entire MicroclimOz dataset. The locations of T1, T2 and T3 are shown for reference.

508 model limitation of plant distribution by multiple nutrients. Again, methods for merging
509 more than two reserves are less well-defined than the two-substrate synthesizing units used
510 in this model.

511 *Process modularity*

512 The model presented in this paper is constructed from generic, open source Julia packages
513 written for this task, but not limited to it. This demonstrates that a high-performance
514 mechanistic model can be composed from generic library components, an approach that
515 has a number of benefits. Common formulations and data sources can become well-tested
516 and canonical, and easily re-purposed for SDMs and other uses. The modular structure
517 also means that varying levels of process complexity can be used to match the processes
518 critical to a particular research question. It can also resolve a criticism of fitted mechanistic
519 models: the assumption that formulations are inherently correct (Dormann et al. 2012).
520 These packages facilitate interactive and automated comparison of multiple formulation
521 combinations, instead of just a single model.

522 The design and interfaces of these modelling tools need to be tested in practical ap-
523 plications and a broader range of contexts. The model as it stands may be useful for
524 general models of the dynamics of vegetation where ontogenetically-explicit environmental
525 responses are frequently limiting. But, an obvious next step is to fit a plant model to specific
526 species or functional types.

527 *Fitting models to species and functional types*

528 Fitting SDMs for plant species of functional types is not without challenges. There is a
529 shortage of suitable data, especially for rare species, and lack of methods for connecting
530 available data and model parameters.

531 To deal with data shortages, it has been suggested that species distribution models
532 should integrate both physiological and observation data into parameter fitting routines
533 (Dormann et al. 2012). Fitting to observations has been demonstrated for mechanistic
534 plant SDMs (Higgins et al. 2012), but methods for combining the uncertainties of observa-
535 tional data and physiological measurements need further work. Bayesian methods may be
536 appropriate for this task (Dormann et al. 2012; Higgins et al. 2012).

537 Another avenue of research involves fitting models to databases of traits and trait-
538 correlations, to specify plant functional types. Model parameters such as rates of reserve
539 turnover, maintenance and resorption, are likely to be correlated with traits (Reich 2014),
540 such as specific leaf area (SLA)). Leaf, stem and seed traits have been demonstrated to
541 be effective species-level predictors of distributions in correlative models (Pollock et al.
542 2012). Mapping DEB model parameters to well-known trait correlations may simplify
543 parameterisation of species-specific models (Wright et al. 2004; Falster et al. 2011).

544 *Optional partitioning and scaling dynamics*

545 In this paper, we have modelled the limitations to growth imposed by microclimatic stresses.
546 But plant growth is also self-limited by changes in the ratio of mass to surface area, and other
547 structural dynamics that cause shifting rates of assimilation, metabolism and translocation
548 over plant ontogeny (Niklas & Hammond 2019). The model presented here used a simple
549 curved response to capture the combined effects of competitively imposed and internal
550 scaling dynamics (Kooijman 2010). This is far from a mechanistic approach, and has many

551 problems, and produces artefacts in root/shoot balance when used over longer lifespans and
552 varying conditions.

553 Mechanistic scaling components such as those outlined in Niklas & Hammond (2019)
554 may improve model behaviour by connecting size related growth dynamics to specific
555 bottom-up processes, rather than top-down formulations imposed by the model. These
556 additions could also include the effects of competition for resources, such as light, water
557 and nutrients, which are not addressed in the model presented here.

558 *Soil water and microclimatic feedbacks*

559 The optimal partitioning dynamics in the model incorporated water availability in shoot
560 assimilation via the stomatal conductance model. But there was no water-dependence
561 for root growth. This may be a critical addition to accurately model optimal root/shoot
562 partitioning for some plants McCarthy & Enquist (2007a).

563 The carbon starvation model of drought stress (O’Grady et al. 2013) was a convenient
564 approach as DEB already tracks C reserves. However, mechanical responses such as hy-
565 draulic failure also contribute to plant mortality. In extreme conditions they may kill a plant
566 without the presence of carbon starvation (Martinez-Vilalta et al. 2019). The interaction
567 of both modes of drought-driven failure may be required for modelling plant distributions
568 constrained by drought stress.

569 In our model, water uptake in photosynthesis and translocation did not strictly observe
570 the conservation of matter: soil water potential in the microclimate is not affected by plant
571 water use. There are multiple feedbacks between vegetation and environment (Billings
572 1952; D’Odorico et al. 2013), but modelling them is difficult. Microclimate calculations can
573 be processor intensive, and introducing plant-environment feedbacks may greatly increase
574 model run-time. The MAESPA model (Duursma & Medlyn 2012) has feedbacks between
575 evapotranspiration and soil water potential, and ultimately radiation, temperature, relative
576 humidity and wind speed should also be influenced by vegetation. Extending microclimate
577 packages like NicheMapR to enable this flexibility while maintaining adequate performance
578 is a challenge for future research.

579 0.6 CONCLUSIONS

580 In this paper we have shown that integrating mechanistic plant growth models with fine-
581 grained microclimate data is a practical option for predicting environmentally forced plant
582 growth dynamics, and ultimately distributions.

583 We have demonstrated methods for connecting dynamic energy budget growth models
584 to microclimate datasets across plant ontogeny. This formulation can produce complex,
585 realistic growth dynamics in response to multiple environmental stresses, and can be scaled
586 up to produce mapped distributions using globally available microclimatic inputs (Kearney
587 et al. 2020).

588 A set of practical modelling libraries has been developed that facilitate the open-ended
589 development of mechanistic species distribution models. Modelling libraries such as these
590 have the potential to make the process of model development more comparable to the effort
591 of producing statistical SDMs.

592 **0.7 ACKNOWLEDGEMENTS**

593 We would like to thank James Maino, Jian Yen, Bas Kooijman, and Daniel Falster for
594 feedback during the development of this manuscript, as well as the reviewers for the detailed
595 feedback provided.

596 0.8 APPENDIX

597 The source code for generating the figures in this paper is available at <https://github.com/rafaqz/DEBplant>. The repository also contains
 598 a script to generate the user interface used to explore the model.

599 The final combination of model parameters are listed in Table. 4, Table. 5, Table. 6. Note that photosynthetic parameters and model
 600 combinations are not particularly meaningful, and serve only as a demonstration of potential to use Farquhar-derived models for this
 601 purpose.

Table 4: DEB parameters, components from DynamicEnergyBudgets.jl

Parameter	Value	Description	Software Component
N_{uptake}	$0.15\mu\text{mol mol}^{-1} \text{s}^{-1}$	Constant rate of N uptake	ConstantNAssim
$y'V_E$	1.0	Yield of structural mass from reserve mass	DEBCore
$y'E_C$	0.9	Yield of general reserve from C-reserve	
$y'E_N$	30.0	Yield of general reserve from N-reserve	
$n'N_V$	0.03	Nitrogen per Carbon in structure	
$n'N_E$	0.025	Nitrogen per Carbon in reserve	
w_V	25.0g mol^{-1}	Mol-weight of shoot structure	
k	0.6d^{-1}	Reserve turnover rate	CatabolismCNshared
$j'E_{mai}$	0.01d^{-1}	Specific somatic maintenance costs	Maintenance
$MV_{ref}S$	0.02mol	Scaling reference for shoots	Plantmorph
$MV_{scaling}S$	0.3mol	Scaling mass for shoots	
$MV_{ref}R$	0.02mol	Scaling reference for roots	Plantmorph
$MV_{scaling}R$	0.3mol	Scaling mass for roots	

Table 5: Non-DEB parameters from DynamicEnergyBudgets.jl

Parameter	Value	Description	Software Component
$K_{resorption}$	1.0e-6	Half saturation metabolic rate for resorption of tissues.	StructuralLossResorption

Parameter	Value	Description	Software Component
ΔH_A	63.5kJ mol ⁻¹	The enthalpy of activation of the reaction. Determines the curvature at low temperature	ParentTardieu
α	3.5	The ratio H_D / H_A	
T_0	300.0K	Reference temperature	
β_{1S}	0.2m	Scalar for conversion to metres	Allometry
α_S	0.2	Exponent relating shoot mass to height	
β_{1R}	1.0m	Scalar for conversion to metres	Allometry
α_R	0.2	Exponent relating root mass to depth	
SLA	24.0m ² kg ⁻¹	Specific leaf area	BallBerryPotentialCAssim

Table 6: C assimilation parameters in Photosynthesis.jl. Adapted from Duursma & Medlyn (2012) and Zhou et al. (2013).

Parameter	Value	Description	Software Component
rdfipt	1.0	Not documented in MAESPA	WangRadiationConductance
tuipt	1.0	Not documented in MAESPA	
tdipt	1.0	Not documented in MAESPA	
leafwidth	0.05 m	Mean width of leaves	BoundaryConductance
gsc	1.0mol m ⁻² s ⁻¹	Stomatal conductance of the boundary layer to CO	
jmax25	184.0 mol m ⁻² s ⁻¹	Maximum rate of electron transport at 25° C	Jmax
delsj	640.02J K ⁻¹ mol ⁻¹	DELTA _S in Medlyn et al. (2002)	
eavj	37259.0J mol ⁻¹	Ha in Medlyn et al. (2002)	
edvj	200000.0J mol ⁻¹	Hd in Medlyn et al. (2002)	
vcmax25	110.0μmol m ⁻² s ⁻¹	Maximumrate rate of rubisco activity at 25° C	NoOptimumVcmax
eavc	47590.0J mol ⁻¹	Ha Medlyn et al. (2002)	
s	2.836MPa ⁻¹	Sensitivity parameter indicating the steepness of the decline	ZhouPotentialDependence
Ψ	-0.958MPa	The water potential at which $f(\Psi_{pd})$ decreases to half of its maximum value	
theta	0.4	Shape of light response curve	RubiscoRegen

Parameter	Value	Description	Software Component
ajq	0.324	Quantum yield of electron transport	
q10f	0.67K^{-1}	Logarithm of the Q10	Respiration
dayresp	0.8	Respiration in the light as fraction of that in the dark	
rd0	$0.01\mu\text{mol m}^{-2} \text{s}^{-1}$	Dark respiration at the reference temperature	
tbelow	173.15K	Temperature below which no respiration occurs	
tref	298.15K	Reference temperature at which rd0 was measured	
g0	$0.5 \mu\text{mol m}^{-2} \text{s}^{-1}$	Stomatal leakiness (gs when photosynthesis is zero)	BallBerryStomatalConductance
gamma	$0.0 \mu\text{mol mol}^{-1}$	Shape parameter of the light response of electron transport	BallBerryGSsubModel
g1	7.0	Slope parameter	
swpexp	0.5kPa^{-1}	Exponent for soil water potential response of stomata	PotentialSoilMethod

602 0.9 MODEL COMPONENT FORMULATIONS

603 All formulation code can be found in DynamicEnergyBudgets.jl. The formulations here
 604 mirror the structure and syntax of the code as much as possible. Flux is tracked for
 605 each root and shoot organ as a matrix with axes state V , C , and N and transformations
 606 *assimilation*, *growth*, *maintenance*, *rejection*, and *resorption*, abbreviated in equations
 607 as *assim*, *grow*, *maint*, *rej* and *res*. Refer to the tables above for parameter descriptions.

608 *Temperature correction*

609 Formulation for from Parent & Tardieu 2012:

$$c = \frac{s_0 T e^{-\frac{\Delta H_A}{RT}}}{1 + \left[e^{-\frac{\Delta H_A}{RT}} \right]^\alpha \left(1 - \frac{T}{T_0} \right)} \quad (4)$$

610 Where T is the current temperature, T_0 is the reference temperature equation, ΔH_A is the
 611 enthalpy of activation, α is the ratio H_D/H_A and R is the gas constant. s_0 is a normalising
 612 constant so that c at T_0 equals 1.

613 *Synthesizing units*

614 The parallel complementary SU is used in this model. See Ledder et al. (2019) for other
 615 possible SUs. k-family and minimum rule SUs are included in DynamicEnergyBudgets.jl.

$$SU_{pc}(v, w) = \frac{vw(v + w)}{v^2 + w^2 + vw} \quad (5)$$

616 *Growth Rate*

617 We calculate the specific growth rate of structure \dot{r} following Kooijman (2010):

$$\dot{r} = y'V, E(\kappa_{soma} \cdot j'E - j'E_{mai}) \quad (6)$$

618 Where:

$$j'E = SU\left(\frac{y'E_C \cdot C(\dot{k}cS - \dot{r})}{V}, \frac{y'E_N \cdot N(\dot{k}cS - \dot{r})}{V}\right) \quad (7)$$

619 Where \dot{k} is the turnover rate, c is the temperature correction, S is the shape scaling factor
 620 and SU is a synthesizing unit function, in our case the Parallel Complimentary SU . This
 621 formulation is not analytically solvable, so a numerical root-finder is used.

622 *Catabolism*

623 Total catabolised general reserve, catabolised general reserve $J'_{E,cat}$ and rejected C and N
 624 reserves are calculated with:

$$catabolism(C, N) = \quad (8)$$

$$J'_{C,cat} = (\dot{k}Sc - \dot{r})C$$

$$J'_{N,cat} = (\dot{k}Sc - \dot{r})N$$

$$J'_{E,cat} = SU(J'_{C,cat}, J'_{N,cat})$$

$$J_{C,rej} = J'_{C,cat} - J'_{E,cat}/y'E_C$$

$$J_{N,rej} = J'_{N,cat} - J'_{E,cat}/y'E_N$$

625 where $J'_{C,cat}$ and $J'_{N,cat}$ are the flux of catabolised C and N reserves, and $J'_{E,cat}$ is the
626 combined catabolised general reserve flux.

627 *Growth*

628 Determine growth fluxes $J_{X,grow}$:

$$growth(V, \dot{r}) = \quad (9)$$

$$J_{V,grow} = \dot{r} * V$$

$$J_{C,grow} = \frac{-J_{V,grow}/y'V_E}{y'E_C}$$

$$J_{N,grow} = \frac{-J_{V,grow}/y'V_E}{y'E_N}$$

629 where \dot{r} is the specific growth rate, V is structure, MV_{ref} is a reference mass and $MV_{scaling}$
630 the scaling mass.

631 *Maintenance*

632 Determine maintenance flux J given state V

$$maintenance(V) = \quad (10)$$

$$J_{C,maint} = \frac{j'E_{maint}Vc}{y'E_C}$$

$$J_{N,maint} = \frac{j'E_{maint}Vc}{y'E_N}$$

633 where c is the temperature correction factor.

634 *Lossless Passive Translocation*

635 Simply translocates the reserve rejected during catabolism between structures:

$$\begin{aligned}
\text{translocation}_L(Jd, Js) &= & (11) \\
Jd_{C,trans} &= -Js_{C,rej} \\
Jd_{N,trans} &= -Js_{N,rej}
\end{aligned}$$

636 where Js and Jd represent shoot and root flux, then root and shoot flux for translocation
637 in the reverse direction.

638 *Dissipative Passive Translocation*

639 This formulation adds parameters for yield of translocation of rejected C and N to reserves,
640 to model overheads of translocation such as the carbon cost of phloem loading. It was not
641 used in the final model, but is illustrative of the modularity of the formulation and ease of
642 comparing parameter/behaviour trade-offs.

$$\begin{aligned}
\text{translocation}_D(Jd, Js) &= & (12) \\
Jd_{C,trans} &= -Js_{C,rej} * y' C_{C,trans} \\
Jd_{N,trans} &= -Js_{N,rej} * y' N_{N,trans}
\end{aligned}$$

643 *Carbon Assimilation*

$$J_{C,asi} = V_S w_V SA(e) \cdot SLA \quad (13)$$

644 Where V_S is shoot structure in moles, w_V is the mass of structure in grams per mole, S is
645 the scaling coefficient, e is the current microclimatic environment, and A is a function that
646 returns the rate of C assimilation. SLA is the specific leaf area of the plant.

647 In this paper a Farquhar von-Caemerer Berry model is used for A . It must be noted
648 that most photosynthesis models calculate the rate of uptake per area, usually extrapolated
649 from total leaf mass. In the DEB formulation, reserve can vary independently to structure,
650 so we use structural mass, not total mass in our calculations. This is because increasing
651 reserve should not directly lead to increased assimilation.

652 *Nitrogen Assimilation*

653 Simple (temperature- and shape-scaled) constant nitrogen assimilation:

$$J_{N,asi} = N_U V_R S \quad (14)$$

654 where N_U is the rate of uptake of N-mols of nitrogen, V_R is root structure S is the shape
655 scaling coefficient.

656 *Organ Metabolism*

$$\text{metabolism}(V, C, N) = (\text{catabolism} \circ \text{maintenance} \circ \text{growth} \circ \text{resorption})(V, C, N) \quad (15)$$

657 Metabolism is calculated for state variables (V_S, C_S, N_S) , then (V_R, C_R, N_R) , for shoot and
658 root organs, and assigned to the flux matrices J_S and J_R respectively.

660 We apply metabolism, translocation and assimilation functions to both root and shoot
661 organs. This formulation allows for the addition of further organs if required.

$$\begin{aligned}
 J_{S1} &= \text{metabolism}(V_S, C_S, N_S) \\
 J_{R1} &= \text{metabolism}(V_R, C_R, N_R) \\
 J_{S2} &= \text{translocation}(J_{R1}, J_{S1}) \\
 J_{R2} &= \text{translocation}(J_{S1}, J_{R1}) \\
 J_{S3} &= \text{assimilation}_C(V_S, V_R) \\
 J_{R3} &= \text{assimilation}_N(V_R, V_S)
 \end{aligned}
 \tag{16}$$

662 Where J_{SN} and J_{RN} are our flux matrices. Finally, state variables (V_S, C_S, N_S) are assigned
663 the sums of all transformations in J_{S3} , and (V_R, C_R, N_R) the sums of all transformations in
664 J_{R3} .

665 0.10 REFERENCES

- 666 Bezanson, J, Karpinski, S, Shah, VB & Edelman, A 2012, ‘Julia : A Fast Dynamic Language for
667 Technical Computing’, accessed October 13, 2017, from <<http://arxiv.org/abs/1209.5145>>.
- 669 Billings, WD 1952, ‘The Environmental Complex in Relation to Plant Growth and Distribution’,
670 *The Quarterly Review of Biology*, vol. 27, no. 3, pp. 251–265, accessed February 24,
671 2019, from <<https://www.journals.uchicago.edu/doi/10.1086/399022>>.
- 672 Bozinovic, F & Pörtner, H-O 2015, ‘Physiological ecology meets climate change’, *Ecology and*
673 *Evolution*, vol. 5, no. 5, pp. 1025–1030, accessed April 9, 2019, from <<http://onlinelibrary.wiley.com/doi/abs/10.1002/ece3.1403>>.
- 675 Cabral, JS, Valente, L & Hartig, F 2017, ‘Mechanistic simulation models in macroecology and
676 biogeography: State-of-art and prospects’, *Ecography*, vol. 40, no. 2, pp. 267–280,
677 accessed October 9, 2017, from <<http://onlinelibrary.wiley.com/doi/10.1111/ecog.02480/abstract>>.
- 679 Caemmerer, S von & Farquhar, GD 1981, ‘Some relationships between the biochemistry of
680 photosynthesis and the gas exchange of leaves’, *Planta*, vol. 153, no. 4, pp. 376–
681 387, accessed August 30, 2017, from <<https://link.springer.com/article/10.1007/BF00384257>>.
- 683 Chapman, DS, Haynes, T, Beal, S, Essl, F & Bullock, JM 2014, ‘Phenology predicts the native
684 and invasive range limits of common ragweed’, *Global Change Biology*, vol. 20, no. 1, pp.
685 192–202, accessed October 8, 2017, from <<http://onlinelibrary.wiley.com/doi/10.1111/gcb.12380/abstract>>.
- 687 Cheeseman, JM 1993, ‘Plant growth modelling without integrating mechanisms’, *Plant, Cell*
688 *& Environment*, vol. 16, no. 2, pp. 137–147, accessed May 9, 2019, from <<http://onlinelibrary.wiley.com/doi/abs/10.1111/j.1365-3040.1993.tb00855.x>>.

- 690 Chuine, I & Beaubien, EG 2001, 'Phenology is a major determinant of tree species range',
691 *Ecology Letters*, vol. 4, no. 5, pp. 500–510, accessed October 8, 2017, from <<http://onlinelibrary.wiley.com/doi/10.1046/j.1461-0248.2001.00261.x/abstract>>.
692
- 693 Connolly, SR, Keith, SA, Colwell, RK & Rahbek, C 2017, 'Process, Mechanism, and Model-
694 ing in Macroecology', *Trends in Ecology & Evolution*, vol. 32, no. 11, pp. 835–844,
695 accessed May 1, 2019, from <<http://www.sciencedirect.com/science/article/pii/S016953471730215X>>.
696
- 697 Dijk, AIJM van, Beck, HE, Crosbie, RS, Jeu, RAM de, Liu, YY, Podger, GM, Timbal, B &
698 Viney, NR 2013, 'The Millennium Drought in southeast Australia (2001–2009): Natural
699 and human causes and implications for water resources, ecosystems, economy, and society',
700 *Water Resources Research*, vol. 49, no. 2, pp. 1040–1057, accessed May 28, 2019, from
701 <<http://agupubs.onlinelibrary.wiley.com/doi/abs/10.1002/wrcr.20123>>.
- 702 D'Odorico, P, He, Y, Collins, S, Wekker, SFJD, Engel, V & Fuentes, JD 2013, 'Vegetation–
703 microclimate feedbacks in woodland–grassland ecotones', *Global Ecology and Biogeog-
704 raphy*, vol. 22, no. 4, pp. 364–379, accessed February 24, 2019, from <<http://onlinelibrary.wiley.com/doi/abs/10.1111/geb.12000>>.
705
- 706 Dormann, CF, Schymanski, SJ, Cabral, J, Chuine, I, Graham, C, Hartig, F, Kearney, M, Morin,
707 X, Römermann, C, Schröder, B & Singer, A 2012, 'Correlation and process in species
708 distribution models: Bridging a dichotomy', *Journal of Biogeography*, vol. 39, no. 12,
709 pp. 2119–2131, accessed September 1, 2017, from <<http://onlinelibrary.wiley.com/doi/10.1111/j.1365-2699.2011.02659.x/abstract>>.
710
- 711 Duursma, RA & Medlyn, BE 2012, 'MAESPA: A model to study interactions between water
712 limitation, environmental drivers and vegetation function at tree and stand levels, with
713 an example application to [CO₂] × drought interactions', *Geosci. Model Dev.*, vol. 5, no.
714 4, pp. 919–940, accessed February 10, 2018, from <<https://www.geosci-model-dev.net/5/919/2012/>>.
715
- 716 Falster, DS, Brännström, Å, Dieckmann, U & Westoby, M 2011, 'Influence of four major plant
717 traits on average height, leaf-area cover, net primary productivity, and biomass density
718 in single-species forests: A theoretical investigation', *Journal of Ecology*, vol. 99, no. 1,
719 pp. 148–164, accessed September 12, 2017, from <<http://onlinelibrary.wiley.com/doi/10.1111/j.1365-2745.2010.01735.x/abstract>>.
720
- 721 Falster, DS, FitzJohn, RG, Brännström, Å, Dieckmann, U & Westoby, M 2016, 'Plant : A package
722 for modelling forest trait ecology and evolution', *Methods in Ecology and Evolution*, vol.
723 7, no. 2, pp. 136–146, accessed September 15, 2017, from <<http://onlinelibrary.wiley.com/doi/10.1111/2041-210X.12525/abstract>>.
724
- 725 Farquhar, GD, Caemmerer, S von & Berry, JA 1980, 'A biochemical model of photosynthetic
726 CO₂ assimilation in leaves of C₃ species', *Planta*, vol. 149, no. 1, pp. 78–90, accessed
727 from <<https://link.springer.com/article/10.1007/BF00386231>>.
- 728 Grimm, V & Berger, U 2016, 'Structural realism, emergence, and predictions in next-generation
729 ecological modelling: Synthesis from a special issue', *Ecological Modelling*, vol. 326,
730 pp. 177–187, accessed October 9, 2017, from <<http://linkinghub.elsevier.com/retrieve/pii/S0304380016000077>>.
731
- 732 Harwood, TD, Mokany, K & Paini, DR 2014, 'Microclimate is integral to the modeling of plant
733 responses to macroclimate', *Proceedings of the National Academy of Sciences*, vol. 111,
734 no. 13, pp. E1164–E1165, accessed February 24, 2019, from <<https://www.pnas.org/content/111/13/E1164>>.
735

- 736 Higgins, SI, O'Hara, RB, Bykova, O, Cramer, MD, Chuine, I, Gerstner, E-M, Hickler, T, Morin,
737 X, Kearney, MR, Midgley, GF & Scheiter, S 2012, 'A physiological analogy of the niche
738 for projecting the potential distribution of plants', *Journal of Biogeography*, vol. 39, no.
739 12, pp. 2132–2145, accessed September 1, 2017, from <<http://onlinelibrary.wiley.com/doi/10.1111/j.1365-2699.2012.02752.x/abstract>>.
- 741 Higgins, SI & Richardson, DM 2014, 'Invasive plants have broader physiological niches', *Proceedings of the National Academy of Sciences*, vol. 111, no. 29, pp. 10610–10614, accessed
742 October 2, 2017, from <<http://www.pnas.org/content/111/29/10610>>.
- 744 Jager, T, Martin, BT & Zimmer, EI 2013, 'DEBkiss or the quest for the simplest generic
745 model of animal life history', *Journal of Theoretical Biology*, vol. 328, pp. 9–18, ac-
746 cessed February 22, 2018, from <<http://linkinghub.elsevier.com/retrieve/pii/S002251931300115X>>.
- 748 Jamieson, PD, Semenov, MA, Brooking, IR & Francis, GS 1998, 'Sirius: A mechanistic model
749 of wheat response to environmental variation', *European Journal of Agronomy*, vol. 8,
750 no. 3, pp. 161–179, accessed May 30, 2019, from <<http://www.sciencedirect.com/science/article/pii/S1161030198000203>>.
- 752 Karban, R 2008, 'Plant behaviour and communication', *Ecology Letters*, vol. 11, no. 7, pp.
753 727–739, accessed December 19, 2018, from <<http://onlinelibrary.wiley.com/doi/abs/10.1111/j.1461-0248.2008.01183.x>>.
- 755 Kearney, M 2012, 'Metabolic theory, life history and the distribution of a terrestrial ectotherm',
756 *Functional Ecology*, vol. 26, no. 1, pp. 167–179, accessed October 9, 2017, from <<http://onlinelibrary.wiley.com/doi/10.1111/j.1365-2435.2011.01917.x/abstract>>.
- 758 Kearney, M & Porter, W 2009, 'Mechanistic niche modelling: Combining physiological and spatial
759 data to predict species' ranges', *Ecology Letters*, vol. 12, no. 4, pp. 334–350, accessed
760 May 1, 2017, from <<http://doi.wiley.com/10.1111/j.1461-0248.2008.01277.x>>.
- 761 Kearney, MR 2018, 'MicroclimOz - A microclimate data set for Australia, with example appli-
762 cations', *Austral Ecology*, accessed March 9, 2019, from <<http://doi.wiley.com/10.1111/aec.12689>>.
- 764 Kearney, MR, Gillingham, PK, Bramer, I, Duffy, JP & Maclean, IMD 2020, 'A method for
765 computing hourly, historical, terrain-corrected microclimate anywhere on earth', *Methods in Ecology and Evolution*, vol. 11, no. 1, pp. 38–43, accessed July 18, 2020, from <<http://besjournals.onlinelibrary.wiley.com/doi/abs/10.1111/2041-210X.13330>>.
- 768 Kearney, MR & Maino, JL 2018, 'Can next-generation soil data products improve soil moisture
769 modelling at the continental scale? An assessment using a new microclimate package
770 for the R programming environment', *Journal of Hydrology*, vol. 561, pp. 662–673, ac-
771 cessed March 8, 2019, from <<http://www.sciencedirect.com/science/article/pii/S0022169418302932>>.
- 773 Kearney, MR & Porter, WP 2017, 'NicheMapR - an R package for biophysical modelling: The
774 microclimate model', *Ecography*, vol. 40, no. 5, pp. 664–674, accessed August 21, 2017,
775 from <<http://doi.wiley.com/10.1111/ecog.02360>>.
- 776 Kearney, MR, Shamakhly, A, Tingley, R, Karoly, DJ, Hoffmann, AA, Briggs, PR & Porter, WP
777 2014, 'Microclimate modelling at macro scales: A test of a general microclimate model
778 integrated with gridded continental-scale soil and weather data' J Travis (ed), *Methods in Ecology and Evolution*, vol. 5, no. 3, pp. 273–286, accessed August 21, 2017, from
779 <<http://doi.wiley.com/10.1111/2041-210X.12148>>.
- 780
- 781 Kearney, MR, Wintle, BA & Porter, WP 2010, 'Correlative and mechanistic models of species

782 distribution provide congruent forecasts under climate change’, *Conservation Letters*, vol.
783 3, no. 3, pp. 203–213, accessed October 9, 2017, from <<http://onlinelibrary.wiley.com/doi/10.1111/j.1755-263X.2010.00097.x/abstract>>.

785 Kitajima, K 2002, ‘Do shade-tolerant tropical tree seedlings depend longer on seed reserves?
786 Functional growth analysis of three Bignoniaceae species’, *Functional Ecology*, vol. 16, no.
787 4, pp. 433–444, accessed January 22, 2019, from <<http://besjournals.onlinelibrary.wiley.com/doi/abs/10.1046/j.1365-2435.2002.00641.x>>.

789 Kooijman, S 2016, ‘DEBtool software’, accessed from <https://www.bio.vu.nl/thb/deb/deblab/debtool/DEBtool_M/manual/>.

791 Kooijman, SALM 1986, ‘What the hen can tell about her eggs: Egg development on the basis of
792 energy budgets’, *Journal of Mathematical Biology*, vol. 23, no. 2, pp. 163–185, accessed
793 May 28, 2019, from <<https://doi.org/10.1007/BF00276955>>.

794 Kooijman, SALM 2010, *Dynamic energy budget theory for metabolic organisation* 3. ed., Cam-
795 bridge Univ. Press, Cambridge.

796 Kooijman, SALM, Andersen, T & Kooi, BW 2004, ‘DYNAMIC ENERGY BUDGET REP-
797 REPRESENTATIONS OF STOICHIOMETRIC CONSTRAINTS ON POPULATION DY-
798 NAMICS’, *Ecology*, vol. 85, no. 5, pp. 1230–1243, accessed May 28, 2019, from
799 <<http://doi.wiley.com/10.1890/02-0250>>.

800 Lambers, H 1983, ‘The functional equilibrium, nibbling on the edges of a paradigm’, *Netherlands*
801 *Journal of Agricultural Science*, vol. 31, pp. 305–311.

802 Ledder, G, Russo, SE, Muller, EB, Peace, A & Nisbet, RM 2019, ‘Local control of resource
803 allocation is sufficient to model optimal dynamics in syntrophic systems’, *bioRxiv*, p.
804 787465, accessed February 28, 2020, from <<https://www.biorxiv.org/content/10.1101/787465v1>>.

806 Levy, PE, Lucas, ME, McKay, HM, Escobar-Gutierrez, AJ & Rey, A 2000, ‘Testing a process-
807 based model of tree seedling growth by manipulating [CO₂] and nutrient uptake’, *Tree*
808 *Physiology*, vol. 20, no. 15, pp. 993–1005, accessed March 23, 2019, from <<https://academic.oup.com/treephys/article/20/15/993/1652862>>.

810 Lorena, A, Marques, GM, Kooijman, SaLM & Sousa, T 2010, ‘Stylized facts in microalgal growth:
811 Interpretation in a dynamic energy budget context’, *Philosophical Transactions of the*
812 *Royal Society of London B: Biological Sciences*, vol. 365, no. 1557, pp. 3509–3521, ac-
813 cessed October 9, 2017, from <<http://rstb.royalsocietypublishing.org/content/365/1557/3509>>.

815 Martinez-Vilalta, J, Anderegg, WRL, Sapes, G & Sala, A 2019, ‘Greater focus on water pools may
816 improve our ability to understand and anticipate drought-induced mortality in plants’,
817 *New Phytologist*, accessed March 5, 2019, from <<http://doi.wiley.com/10.1111/nph.15644>>.

819 Mccarthy, MC & Enquist, BJ 2007a, ‘Consistency between an allometric approach and optimal
820 partitioning theory in global patterns of plant biomass allocation’, *Functional Ecology*,
821 vol. 21, no. 4, pp. 713–720, accessed September 1, 2017, from <<http://onlinelibrary.wiley.com/doi/10.1111/j.1365-2435.2007.01276.x/abstract>>.

823 Mccarthy, MC & Enquist, BJ 2007b, ‘Consistency between an allometric approach and optimal
824 partitioning theory in global patterns of plant biomass allocation’, *Functional Ecology*,
825 vol. 21, no. 4, pp. 713–720, accessed December 22, 2018, from <<http://besjournals.onlinelibrary.wiley.com/doi/abs/10.1111/j.1365-2435.2007.01276.x>>.

- 827 McConnaughay, KDM & Coleman, JS 1999a, ‘Biomass Allocation in Plants: Ontogeny or Opti-
828 mality? A Test Along Three Resource Gradients’, *Ecology*, vol. 80, no. 8, pp. 2581–2593,
829 accessed December 15, 2018, from <[https://esajournals.onlinelibrary.wiley.com/
830 doi/abs/10.1890/0012-9658%281999%29080%5B2581%3ABAIP00%5D2.0.CO%3B2](https://esajournals.onlinelibrary.wiley.com/doi/abs/10.1890/0012-9658%281999%29080%5B2581%3ABAIP00%5D2.0.CO%3B2)>.
- 831 McConnaughay, KDM & Coleman, JS 1999b, ‘Biomass Allocation in Plants: Ontogeny or Opti-
832 mality? A Test Along Three Resource Gradients’, *Ecology*, vol. 80, no. 8, pp. 2581–2593,
833 accessed April 29, 2019, from <[http://esajournals.onlinelibrary.wiley.com/doi/
834 abs/10.1890/0012-9658%281999%29080%5B2581%3ABAIP00%5D2.0.CO%3B2](http://esajournals.onlinelibrary.wiley.com/doi/abs/10.1890/0012-9658%281999%29080%5B2581%3ABAIP00%5D2.0.CO%3B2)>.
- 835 Merow, C, LaFleur, N, Silander Jr., JA, Wilson, AM & Rubega, M 2011, ‘Developing Dynamic
836 Mechanistic Species Distribution Models: Predicting Bird-Mediated Spread of Invasive
837 Plants across Northeastern North America.’, *The American Naturalist*, vol. 178, no. 1,
838 pp. 30–43, accessed October 5, 2017, from <[http://www.journals.uchicago.edu/doi/
839 abs/10.1086/660295](http://www.journals.uchicago.edu/doi/abs/10.1086/660295)>.
- 840 Metcalfe, DB, Meir, P, Aragão, LEOC, da Costa, ACL, Braga, AP, Gonçalves, PHL, de Athaydes
841 Silva Junior, J, de Almeida, SS, Dawson, LA, Malhi, Y & Williams, M 2008, ‘The effects
842 of water availability on root growth and morphology in an Amazon rainforest’, *Plant and
843 Soil*, vol. 311, no. 1, pp. 189–199, accessed March 6, 2019, from <[https://doi.org/10.
844 1007/s11104-008-9670-9](https://doi.org/10.1007/s11104-008-9670-9)>.
- 845 Michaletz, ST, Weiser, MD, Zhou, J, Kaspari, M, Helliker, BR & Enquist, BJ 2015, ‘Plant
846 Thermoregulation: Energetics, Trait–Environment Interactions, and Carbon Economics’,
847 *Trends in Ecology & Evolution*, vol. 30, no. 12, pp. 714–724, accessed December 19, 2018,
848 from <<http://www.sciencedirect.com/science/article/pii/S0169534715002396>>.
- 849 Moncrieff, GR, Scheiter, S, Langan, L, Trabucco, A & Higgins, SI 2016, ‘The future distribution
850 of the savannah biome: Model-based and biogeographic contingency’, *Phil. Trans. R.
851 Soc. B*, vol. 371, no. 1703, p. 20150311, accessed October 2, 2017, from <[http:
852 //rstb.royalsocietypublishing.org/content/371/1703/20150311](http://rstb.royalsocietypublishing.org/content/371/1703/20150311)>.
- 853 Morin, X, Viner, D & Chuine, I 2008, ‘Tree species range shifts at a continental scale: New
854 predictive insights from a process-based model’, *Journal of Ecology*, vol. 96, no. 4,
855 pp. 784–794, accessed December 22, 2018, from <[http://besjournals.onlinelibrary.
856 wiley.com/doi/abs/10.1111/j.1365-2745.2008.01369.x](http://besjournals.onlinelibrary.wiley.com/doi/abs/10.1111/j.1365-2745.2008.01369.x)>.
- 857 Muller, EB, Kooijman, SALM, Edmunds, PJ, Doyle, FJ & Nisbet, RM 2009, ‘Dynamic energy
858 budgets in syntrophic symbiotic relationships between heterotrophic hosts and photoau-
859 totrophic symbionts’, *Journal of Theoretical Biology*, vol. 259, no. 1, pp. 44–57, ac-
860 cessed May 10, 2019, from <[http://www.sciencedirect.com/science/article/pii/
861 S002251930900109X](http://www.sciencedirect.com/science/article/pii/S002251930900109X)>.
- 862 Müller, I, Schmid, B & Weiner, J 2000, ‘The effect of nutrient availability on biomass allocation
863 patterns in 27 species of herbaceous plants’, *Perspectives in Plant Ecology, Evolution
864 and Systematics*, vol. 3, no. 2, pp. 115–127, accessed May 30, 2019, from <[http:
865 //www.sciencedirect.com/science/article/pii/S1433831904700323](http://www.sciencedirect.com/science/article/pii/S1433831904700323)>.
- 866 Munné-Bosch, S & Alegre, L 2004, ‘Die and let live: Leaf senescence contributes to plant survival
867 under drought stress’, *Functional Plant Biology*, vol. 31, no. 3, pp. 203–216, accessed
868 May 17, 2019, from <<http://www.publish.csiro.au/fp/FP03236>>.
- 869 Nabout, JC, Caetano, JM, Ferreira, RB, Teixeira, IR & Alves, SM de F 2012, ‘Using correlative,
870 mechanistic and hybrid niche models to predict the productivity and impact of global
871 climate change on maize crop in Brazil’, *Natureza & Conservação*, vol. 10, no. 2, pp.
872 177–183, accessed October 9, 2017, from <[http://doi.editoracubo.com.br/10.4322/
873 natcon.2012.034](http://doi.editoracubo.com.br/10.4322/natcon.2012.034)>.

- 874 Niinemets, Ü 2010, ‘Responses of forest trees to single and multiple environmental stresses
875 from seedlings to mature plants: Past stress history, stress interactions, tolerance and
876 acclimation’, *Forest Ecology and Management*, vol. 260, no. 10, pp. 1623–1639, ac-
877 cessed March 18, 2019, from <[http://www.sciencedirect.com/science/article/pii/
878 S0378112710004743](http://www.sciencedirect.com/science/article/pii/S0378112710004743)>.
- 879 Niklas, KJ & Hammond, ST 2019, ‘Biophysical Effects on the Scaling of Plant Growth, Form,
880 and Ecology’, *Integrative and Comparative Biology*, vol. 59, no. 5, pp. 1312–1323, ac-
881 cessed February 24, 2020, from <[http://academic.oup.com/icb/article/59/5/1312/
882 5487414](http://academic.oup.com/icb/article/59/5/1312/5487414)>.
- 883 O’Grady, AP, Mitchell, PJM, Pinkard, EA & Tissue, DT 2013, ‘Thirsty roots and hungry leaves:
884 Unravelling the roles of carbon and water dynamics in tree mortality’, *New Phytologist*,
885 vol. 200, no. 2, pp. 294–297, accessed March 15, 2018, from <[http://onlinelibrary.
886 wiley.com/doi/10.1111/nph.12451/abstract](http://onlinelibrary.wiley.com/doi/10.1111/nph.12451/abstract)>.
- 887 Parent, B & Tardieu, F 2012, ‘Temperature responses of developmental processes have not been
888 affected by breeding in different ecological areas for 17 crop species’, *New Phytologist*,
889 vol. 194, no. 3, pp. 760–774, accessed October 9, 2017, from <[http://onlinelibrary.
890 wiley.com/doi/10.1111/j.1469-8137.2012.04086.x/abstract](http://onlinelibrary.wiley.com/doi/10.1111/j.1469-8137.2012.04086.x/abstract)>.
- 891 Perrin, N 1992, ‘Optimal Resource Allocation and the Marginal Value of Organs’, *The American
892 Naturalist*, vol. 139, no. 6, pp. 1344–1369, accessed May 9, 2019, from <[https://www.
893 jstor.org/stable/2462345](https://www.jstor.org/stable/2462345)>.
- 894 Pollock, LJ, Morris, WK & Vesk, PA 2012, ‘The role of functional traits in species distribu-
895 tions revealed through a hierarchical model’, *Ecography*, vol. 35, no. 8, pp. 716–725,
896 accessed July 20, 2020, from <[http://onlinelibrary.wiley.com/doi/abs/10.1111/
897 j.1600-0587.2011.07085.x](http://onlinelibrary.wiley.com/doi/abs/10.1111/j.1600-0587.2011.07085.x)>.
- 898 Postma, JA, Kuppe, C, Owen, MR, Mellor, N, Griffiths, M, Bennett, MJ, Lynch, JP & Watt, M
899 2017, ‘OpenSimRoot: Widening the scope and application of root architectural models’,
900 *New Phytologist*, vol. 215, no. 3, pp. 1274–1286, accessed July 18, 2020, from <[http:
901 //nph.onlinelibrary.wiley.com/doi/abs/10.1111/nph.14641](http://nph.onlinelibrary.wiley.com/doi/abs/10.1111/nph.14641)>.
- 902 reichert, p & omlin, m 1997, ‘on the usefulness of overparameterized ecological models’, *ecological
903 modelling*, vol. 95, no. 2, pp. 289–299, accessed may 10, 2019, from <[http://www.
904 sciencedirect.com/science/article/pii/S0304380096000439](http://www.sciencedirect.com/science/article/pii/S0304380096000439)>.
- 905 Reich, PB 2014, ‘The world-wide “fast–slow” plant economics spectrum: A traits manifesto’,
906 *Journal of Ecology*, vol. 102, no. 2, pp. 275–301, accessed July 20, 2020, from <[http:
907 //besjournals.onlinelibrary.wiley.com/doi/abs/10.1111/1365-2745.12211](http://besjournals.onlinelibrary.wiley.com/doi/abs/10.1111/1365-2745.12211)>.
- 908 Sánchez-Salguero, R, Camarero, JJ, Gutiérrez, E, Rouco, FG, Gazol, A, Sangüesa-Barreda, G,
909 Andreu-Hayles, L, Linares, JC & Seftigen, K 2016, ‘Assessing forest vulnerability to
910 climate warming using a process-based model of tree growth: Bad prospects for rear-
911 edges’, *Global Change Biology*, vol. 23, no. 7, pp. 2705–2719, accessed July 16, 2018,
912 from <<http://onlinelibrary.wiley.com/doi/abs/10.1111/gcb.13541>>.
- 913 Sarà, G, Palmeri, V, Montalto, V, Rinaldi, A & Widdows, J 2013, ‘Parameterisation of bivalve
914 functional traits for mechanistic eco-physiological dynamic energy budget (DEB) models’,
915 *Marine Ecology Progress Series*, vol. 480, pp. 99–117, accessed October 5, 2017, from
916 <<http://www.int-res.com/abstracts/meps/v480/p99-117/>>.
- 917 Singer, A, Johst, K, Banitz, T, Fowler, MS, Groeneveld, J, Gutiérrez, AG, Hartig, F, Krug, RM,
918 Liess, M, Matlack, G, Meyer, KM, Pe’er, G, Radchuk, V, Voinopol-Sassu, A-J & Travis,
919 JMJ 2016, ‘Community dynamics under environmental change: How can next generation

- 920 mechanistic models improve projections of species distributions?', *Ecological Modelling*,
 921 vol. 326, pp. 63–74, accessed December 22, 2018, from <<http://www.sciencedirect.com/science/article/pii/S0304380015005281>>.
- 923 Smith, WK, Germino, MJ, Johnson, DM & Reinhardt, K 2009, 'The Altitude of Alpine Treeline:
 924 A Bellwether of Climate Change Effects', *The Botanical Review*, vol. 75, no. 2, pp. 163–
 925 190, accessed February 21, 2019, from <<https://doi.org/10.1007/s12229-009-9030-3>>.
- 926 Sousa, T, Domingos, T, Poggiale, J-C & Kooijman, SaLM 2010, 'Dynamic energy budget theory
 927 restores coherence in biology', *Philosophical Transactions of the Royal Society of London
 928 B: Biological Sciences*, vol. 365, no. 1557, pp. 3413–3428, accessed from <<http://rstb.royalsocietypublishing.org/content/365/1557/3413>>.
- 930 Storkey, J, Stratonovitch, P, Chapman, DS, Vidotto, F & Semenov, MA 2014, 'A Process-
 931 Based Approach to Predicting the Effect of Climate Change on the Distribution of
 932 an Invasive Allergenic Plant in Europe', *PLOS ONE*, vol. 9, no. 2, p. e88156, ac-
 933 cessed February 21, 2019, from <<https://journals.plos.org/plosone/article?id=10.1371/journal.pone.0088156>>.
- 935 Stratonovitch, P, Storkey, J & Semenov, MA 2012, 'A process-based approach to modelling im-
 936 pacts of climate change on the damage niche of an agricultural weed', *Global Change Biol-
 937 ogy*, vol. 18, no. 6, pp. 2071–2080, accessed May 22, 2019, from <<http://onlinelibrary.wiley.com/doi/abs/10.1111/j.1365-2486.2012.02650.x>>.
- 939 Thornley, JHM 1972a, 'A Balanced Quantitative Model for Root: Shoot Ratios in Vegetative
 940 Plants', *Annals of Botany*, vol. 36, no. 145, pp. 431–441, accessed from <<http://www.jstor.org/stable/42753756>>.
- 942 Thornley, JHM 1972b, 'A Model to Describe the Partitioning of Photosynthate during Vegetative
 943 Plant Growth', *Annals of Botany*, vol. 36, no. 145, pp. 419–430, accessed from <<http://www.jstor.org/stable/42753755>>.
- 945 Vergutz, L, Manzoni, S, Porporato, A, Novais, RF & Jackson, RB 2012, 'Global resorption
 946 efficiencies and concentrations of carbon and nutrients in leaves of terrestrial plants',
 947 *Ecological Monographs*, vol. 82, no. 2, pp. 205–220, accessed May 10, 2019, from <<http://esajournals.onlinelibrary.wiley.com/doi/abs/10.1890/11-0416.1>>.
- 949 Vrugt, JA, Wijk, MT van, Hopmans, JW & Šimunek, J 2001, 'One-, two-, and three-dimensional
 950 root water uptake functions for transient modeling', *Water Resources Research*, vol. 37,
 951 no. 10, pp. 2457–2470, accessed May 13, 2019, from <<http://agupubs.onlinelibrary.wiley.com/doi/abs/10.1029/2000WR000027>>.
- 953 Wright, IJ, Reich, PB, Westoby, M, Ackerly, DD & al, et 2004, 'The worldwide leaf economics
 954 spectrum', *Nature; London*, vol. 428, no. 6985, pp. 821–7, accessed August 31, 2017, from
 955 <<https://search.proquest.com/docview/204538159/abstract/803B1F65299B4C57PQ/1>>.
- 957 Wright, IJ & Westoby, M 2003, 'Nutrient concentration, resorption and lifespan: Leaf traits of
 958 Australian sclerophyll species', *Functional Ecology*, vol. 17, no. 1, pp. 10–19, accessed
 959 April 17, 2019, from <<http://besjournals.onlinelibrary.wiley.com/doi/abs/10.1046/j.1365-2435.2003.00694.x>>.
- 961 Zhou, S, Duursma, RA, Medlyn, BE, Kelly, JWG & Prentice, IC 2013, 'How should we model
 962 plant responses to drought? An analysis of stomatal and non-stomatal responses to water
 963 stress', *Agricultural and Forest Meteorology*, vol. 182–183, pp. 204–214, accessed February
 964 3, 2019, from <<http://www.sciencedirect.com/science/article/pii/S0168192313001263>>.